

Low- x contribution to the Bjorken sum rule within unified ln^2x +LO DGLAP approximation

DOROTA KOTLORZ ¹, ANDRZEJ KOTLORZ ²

¹Department of Physics Ozimska 75, ²Department of Mathematics Luboszycka 3,
 Technical University of Opole, 45-370 Opole, Poland, e-mail ¹:
 dstrozik@po.opole.pl

The small- x contributions to the Bjorken sum rule within unified picture ln^2x +LO DGLAP for different input parametrisations $g_1^{NS}(x, Q_0^2)$ are presented. Theoretical predictions for $\int_0^{0.003} g_1^{NS}(x, Q^2 = 10) dx$ are compared with the SMC small- x data. Rough estimation of the slope λ , controlling the small- x behaviour of $g_1^{NS} \sim x^{-\lambda}$ from the obtained results and SMC data is performed. The crucial role of the running coupling $\alpha_s = \alpha_s(Q^2/z)$ at low- x is taken into account.

PACS numbers: 12.38 Bx

1. Introduction

The results of SIDIS (semi inclusive deep inelastic scattering) experiments with polarised beams and targets enable the extraction of the spin dependent quark and gluon densities. This powerful tool of studying the internal spin structure of the nucleon allows verification of sum rules. One of them is the Bjorken sum rule (BSR) [1], which refers to the first moment of the nonsinglet spin dependent structure function $g_1^{NS}(x, Q^2)$. Because of $SU_f(2)$ flavour symmetry, BSR is regarded as exact. Thus all of estimations of polarised parton distributions should be performed under the assumption that the BSR is valid. Determination of the sum rules requires knowledge of spin dependent structure functions over the entire region of $x \in (0; 1)$. The experimentally accessible x range for the spin dependent DIS is however limited ($0.7 > x > 0.003$ for SMC data [2]) and therefore one should extrapolate results to $x = 0$ and $x = 1$. The extrapolation to $x \rightarrow 0$, where structure functions grow strongly, is much more important than the extrapolation to $x \rightarrow 1$, where structure functions vanish. Assuming that the BSR is valid, one can determinate from existing experimental data the very

small- x contribution ($0.003 > x > 0$) to the sum rule. Theoretical analysis of the small- x behaviour of $g_1^{NS}(x, Q^2) = g_1^p(x, Q^2) - g_1^n(x, Q^2)$ together with the broad x -range measurement data allow verification of the shape of the input parton distributions. In this way one can determinate the free parameters in these input distributions. Experimental data confirm the theoretical predictions of the singular small- x behaviour of the polarised structure functions. It is well known, that the low- x behaviour of both unpolarised and polarised structure functions is controlled by the double logarithmic terms $(\alpha_s \ln^2 x)^n$ [3],[4]. For the unpolarised case, this singular PQCD behaviour is however overridden by the leading Regge contribution [5]. Therefore, the double logarithmic approximation is very important particularly for the spin dependent structure function g_1 . The resummation of the $\ln^2 x$ terms at low x goes beyond the standard LO and NLO PQCD evolution of the parton densities. The nonsinglet polarised structure function g_1^{NS} , governed by leading $\alpha_s^n \ln^{2n} x$ terms, is a convenient function both for theoretical analysis (because of its simplicity) and for the experimental BSR tests. The small- x behaviour of g_1^{NS} implied by double logarithmic approximation has a form $x^{-\lambda}$ with $\lambda \approx 0.4$. This or similar small- x extrapolation of the spin dependent quark distributions have been assumed in recent input parametrisations e.g. in [6],[7],[13]. More singular parametrisation of $g_1^{0NS}(x, Q_0^2 = 4) \sim x^{-0.8}$ at small- x , based on the QCD (LO and NLO) analysis of the world data on polarised deep inelastic scattering, has been presented in [14]. Mentioned above double logarithmic approach is however inaccurate for QCD analysis at medium and large values of x . Therefore the double logarithmic approximation should be completed by LO DGLAP Q^2 evolution. In our theoretical analysis within $\ln^2 x$ +LO DGLAP approach we estimate g_1^{NS} at low- x and hence the small- x contributions $\int_0^{x_0} g_1^{NS}(x, Q^2) dx$, $\int_{x_1}^{x_2} g_1^{NS}(x, Q^2) dx$ ($x_0, x_1, x_2 \ll 1$) to the BSR for different input quark parametrisations: the Regge nonsingular one and the singular one. We compare our results with the suitable experimental SMC data for BSR. In the next section we recall some of the recent theoretical developments concerning the small- x behaviour of the nonsinglet polarised structure function g_1^{NS} . Section 3 is devoted to the presentation of the unified $\ln^2 x$ +LO DGLAP approximation. We also discuss the role of the running coupling α_s . Section 4 contains our results for the structure function g_1^{NS} at small- x and for contributions to the Bjorken sum rule $\Delta I_{BSR}(x_1, x_2, Q^2) = \int_{x_1}^{x_2} g_1^{NS}(x, Q^2) dx$ ($x_1, x_2 \ll 1$). We present our predictions using flat (nonsingular) $\sim (1-x)^3$ and singular $\sim x^{-\lambda}$ at small- x parametrisations of the input structure function $g_1^{NS}(x, Q_0^2)$ as well. We compare our results with the SMC data for the small- x contribution to the BSR. We roughly estimate the slope λ controlling the small- x behaviour of $g_1^{NS} \sim x^{-\lambda}$ from our g_1^{NS} predictions and from the SMC data, basing

on the validity of the BSR. We compare also results $\Delta I_{BSR}(x_1, x_2, Q^2)$ and $g_1^{NS}(x = 10^{-6}, Q^2 = 10)$ in different approximations: pure LO DGLAP, pure $\ln^2 x$, $\ln^2 x + \text{LO DGLAP}$ and obtained for different α_s parametrisations: $\alpha_s = \text{const}$, $\alpha_s = \alpha_s(Q^2)$, $\alpha_s = \alpha_s(Q^2/z)$. Finally, Section 5 contains a summary of our paper.

2. Small- x behaviour of the nonsinglet spin dependent structure function $g_1^{NS}(x, Q^2)$

The small value of the Bjorken parameter x , specifying the longitudinal momentum fraction of a hadron carried by a parton, corresponds by definition to the Regge limit ($x \rightarrow 0$). Therefore the small- x behaviour of structure functions can be described using the Regge pole exchange model [5]. In this model the spin dependent nonsinglet structure function $g_1^{NS} = g_1^p - g_1^n$ in the low- x region behave as:

$$g_1^{NS}(x, Q^2) = \gamma(Q^2)x^{-\alpha_{A_1}(0)} \quad (2.1)$$

where $\alpha_{A_1}(0)$ is the intercept of the A_1 Regge pole trajectory, corresponding to the axial vector meson and lies in the limits

$$-0.5 \leq \alpha_{A_1}(0) \leq 0 \quad (2.2)$$

This low value of the intercept (2.2) implies the nonsingular, flat behaviour of the g_1^{NS} function at small- x . The nonperturbative contribution of the A_1 Regge pole is however overridden by the perturbative QCD contributions, particularly by resummation of double logarithmic terms $\ln^2 x$. In this way the Regge behaviour of the spin dependent structure functions is unstable against the perturbative QCD expectations, which at low- x generate more singular x dependence than that implied by (2.1)-(2.2). Nowadays it is well known that the small- x behaviour of the nonsinglet polarised structure function g_1^{NS} is governed by the double logarithmic terms i.e. $(\alpha_s \ln^2 x)^n$ [3],[4]. Effects of these $\ln^2 x$ approach go beyond the standard LO and even NLO Q^2 evolution of the spin dependent parton distributions and significantly modify the Regge pole model expectations for the structure functions. From the recent theoretical analyses of the low- x behaviour of the g_1^{NS} function [9] one can find that resummation of the double logarithmic terms $(\alpha_s \ln^2 x)^n$ leads to the singular form:

$$g_1^{NS}(x, Q^2) \sim x^{-\lambda} \quad (2.3)$$

with $\lambda \approx 0.4$. This behaviour of g_1^{NS} is well confirmed by experimental data, after a low- x extrapolation beyond the measured region [2],[10],[11].

3. Unintegrated structure function $f^{NS}(x, Q^2)$ within double logarithmic $\ln^2 x$ and unified $\ln^2 x + \text{LO DGLAP}$ approximations

Perturbative QCD predicts a strong increase of the structure function $g_1^{NS}(x, Q^2)$ with the decreasing parameter x [3],[4] what is confirmed by experimental data [2],[10],[11]. This growth is implied by resummation of $\ln^2 x$ terms in the perturbative expansion. The double logarithmic effects come from the ladder diagram with quark and gluon exchanges along the chain. In this approximation the unintegrated nonsinglet structure function $f^{NS}(x, Q^2)$ satisfies the following integral evolution equation [3]:

$$f^{NS}(x, Q^2) = f_0^{NS}(x) + \int_x^1 \frac{dz}{z} \int_{Q_0^2}^{Q^2/z} \frac{dk'^2}{k'^2} \bar{\alpha}_s f^{NS}\left(\frac{x}{z}, k'^2\right) \quad (3.1)$$

where

$$\bar{\alpha}_s = \frac{2\alpha_s}{3\pi} \quad (3.2)$$

and $f_0^{NS}(x)$ is a nonperturbative contribution which has a form:

$$f_0^{NS}(x) = \bar{\alpha}_s \int_x^1 \frac{dz}{z} g_1^{0NS}(z) \quad (3.3)$$

$g_1^{0NS}(x)$ is an input parametrisation

$$g_1^{0NS}(x) = g_1^{NS}(x, Q^2 = Q_0^2) \quad (3.4)$$

The unintegrated distribution $f^{NS}(x, Q^2)$ is related to the $g_1^{NS}(x, Q^2)$ via

$$f^{NS}(x, Q^2) = \frac{\partial g_1^{NS}(x, Q^2)}{\partial \ln Q^2} \quad (3.5)$$

Eq. (3.1) generates the leading small- x behaviour of f^{NS} and hence g_1^{NS} , but it is inaccurate in describing the total Q^2 evolution. For larger values of x , which are involved in the evolution equation (3.1) via $\int_x^1 dz$ one should take into account Q^2 DGLAP evolution with complete splitting function $P_{qq}(z)$. Therefore the double logarithmic approach should be completed by LO DGLAP Q^2 evolution. Unified description of the polarised structure function $f^{NS}(x, Q^2)$ incorporating DGLAP evolution and the double

logarithmic $\ln^2 x$ effects at low- x leads to the following equation for the unintegrated distribution $f^{NS}(x, Q^2)$ [18]:

$$\begin{aligned}
f^{NS}(x, Q^2) &= f_0^{NS}(x) + \int_x^1 \frac{dz}{z} \int_{Q^2}^{Q^2/z} \frac{dk'^2}{k'^2} \bar{\alpha}_s f\left(\frac{x}{z}, k'^2\right) \\
&+ \int_{Q_0^2}^{Q^2} \frac{dk'^2}{k'^2} \int_x^1 \frac{dz}{z} \bar{\alpha}_s \frac{(1+z^2)f(x/z, k'^2) - 2zf(x, k'^2)}{1-z} \\
&+ \bar{\alpha}_s \int_{Q_0^2}^{Q^2} \frac{dk'^2}{k'^2} \left(\frac{3}{2} + 2\ln(1-x)\right) f(x, k'^2)
\end{aligned} \tag{3.6}$$

where

$$\begin{aligned}
f_0^{NS}(x) &= \bar{\alpha}_s \left[\int_x^1 \frac{dz}{z} \frac{(1+z^2)g_1^{(0)}(x/z) - 2zg_1^{(0)}(x)}{1-z} \right. \\
&\left. + \left(\frac{3}{2} + 2\ln(1-x)\right) g_1^{(0)}(x) \right]
\end{aligned} \tag{3.7}$$

The unintegrated distribution f^{NS} in the equation (3.6) is related to the $g_1^{NS}(x, Q^2)$ via

$$g_1^{NS}(x, Q^2) = g_1^{0NS}(x) + \int_{Q_0^2}^{Q^2(1/x-1)} \frac{dk^2}{k^2} f\left(x\left(1 + \frac{k^2}{Q^2}\right), k^2\right) \tag{3.8}$$

An important role in solutions of (3.1) and (3.6) plays the coupling α_s , which can be parametrised in different way. The simplest choice of α_s is a constance (nonrunning) coupling:

$$\alpha_s = \text{const} \tag{3.9}$$

This simplification allows the analytical analysis of the suitable evolution equations for truncated and full moments of the unintegrated structure function $f^{NS}(x, Q^2)$ within $\ln^2 x$ approximation [3],[8]. The introduction of the running coupling effects implies α_s in (3.1) and (3.6) of a form

$$\alpha_s = \alpha_s(Q^2) \tag{3.10}$$

It has been however lately proved [9], that dealing with a very small- x region one should use a prescription for the running coupling in a form $\alpha_s =$

$\alpha_s(Q^2/z)$. This parametrisation is theoretically more justified than $\alpha_s = \alpha_s(Q^2)$. Namely, the substitution $\alpha_s = \alpha_s(Q^2)$ is valid only for hard QCD processes, when $x \sim 1$. However the evolution of DIS structure functions at small- x needs "more running" α_s :

$$\alpha_s = \alpha_s(Q^2/z) \quad (3.11)$$

Our predictions for g_1^{NS} and $\Delta I_{BSR}(x_1, x_2, Q^2)$ for different forms of α_s will be presented in the forthcoming section.

4. Predictions for g_1^{NS} and small- x contribution to the BSR

Our purpose is to calculate the nonsinglet polarised structure function $g_1^{NS}(x, Q^2)$ and hence also the contribution to the Bjorken sum rule in the small- x region. The BSR is a fundamental rule and must hold as a rigorous prediction of QCD in the limit of the infinite momentum transfer Q^2 :

$$I_{BSR} \equiv \Gamma_1^p - \Gamma_1^n = \int_0^1 dx g_1^{NS}(x, Q^2) = \frac{1}{6} \left| \frac{g_A}{g_V} \right| \quad (4.1)$$

where

$$\Gamma_1^p \equiv \int_0^1 dx g_1^p(x, Q^2) \quad (4.2)$$

$$\Gamma_1^n \equiv \int_0^1 dx g_1^n(x, Q^2) \quad (4.3)$$

and $|\frac{g_A}{g_V}|$ is the neutron β -decay constant

$$\left| \frac{g_A}{g_V} \right| = F + D = 1.2670 \quad (4.4)$$

Hence the BSR for the flavour symmetric sea quarks scenario ($\Delta\bar{u} = \Delta\bar{d}$) reads:

$$I_{BSR}(Q^2) \equiv \int_0^1 dx g_1^{NS}(x, Q^2) \approx 0.211 \quad (4.5)$$

The small- x contribution to the BSR has a form:

$$\Delta I_{BSR}(x_1, x_2, Q^2) \equiv \int_{x_1}^{x_2} dx g_1^{NS}(x, Q^2) \quad (4.6)$$

Below we present our results for g_1^{NS} and ΔI_{BSR} at small- x obtained for different α_s sets (3.9)-(3.11) within combined $\ln^2 x + \text{LO}$ DGLAP approach. We compare these predictions with pure LO DGLAP and pure $\ln^2 x$ results as well. We solve numerically the evolution equation (3.6) in a case of unified $\ln^2 x + \text{LO}$ DGLAP picture and in a case of pure LO DGLAP, when one gets the following equation:

$$f^{NS}(x, Q^2) = f_0^{NS}(x) + \int_{Q_0^2}^{Q^2} \frac{dk'^2}{k'^2} \int_x^1 \frac{dz}{z} \bar{\alpha}_s \frac{(1+z^2)f(x/z, k'^2) - 2zf(x, k'^2)}{1-z} + \bar{\alpha}_s \int_{Q_0^2}^{Q^2} \frac{dk'^2}{k'^2} \left(\frac{3}{2} + 2 \ln(1-x) \right) f(x, k'^2) \quad (4.7)$$

In order to have comparable results, for pure $\ln^2 x$ analysis we also use numerical solutions of (3.1). Our predictions have been found for two different input parametrisations $g_1^{0NS}(x)$, chosen at $Q_0^2 = 1 \text{ GeV}^2$:

$$1. \quad g_1^{0NS}(x) = 0.8447(1-x)^3 \quad (4.8)$$

$$2. \quad g_1^{0NS}(x) = 0.290x^{-0.4}(1-x)^{2.5} \quad (4.9)$$

Input 1 is the simple Regge form, constance as $x \rightarrow 0$; input 2 is a "toy" model, in which we have used the latest theoretical results concerning the small- x behaviour $x^{-0.4}$ of the nonsinglet function g_1^{NS} [9]. In Fig.1 we plot inputs $g_1^{0NS}(x)$ (4.8)- (4.9) in the low- x region [$10^{-5} \div 10^{-2}$] together with $g_1^{NS}(x, Q^2)$ results for $Q^2 = 10 \text{ GeV}^2$ within $\ln^2 x + \text{LO}$ DGLAP approach with "very running" coupling $\alpha_s = \alpha_s(Q^2/z)$. Fig.2 contains comparison of three approximations: pure $\ln^2 x$, pure LO DGLAP and unified $\ln^2 x + \text{LO}$ DGLAP. We present structure function $g_1^{NS}(x, Q^2 = 10)$ for $\alpha_s = \alpha_s(Q^2/z)$. Finally, Fig.3 shows the $g_1^{NS}(x, Q^2 = 10)$ results within combined $\ln^2 x + \text{LO}$ DGLAP approach for different parametrisations of α_s : (3.9)-(3.11). In each figure we present the solutions for both input parametrisations (4.8)-(4.9). Numbers at each plot correspond to the suitable inputs 1 or 2. In Table I we present our results for the low- x contributions to the BSR (4.6) together with $\varepsilon(x_1, x_2)$, which is defined by the following expression:

$$\int_{x_1}^{x_2} dx g_1^{NS}(x, Q^2) = [1 + \varepsilon(x_1, x_2)] \int_{x_1}^{x_2} dx g_1^{0NS}(x) \quad (4.10)$$

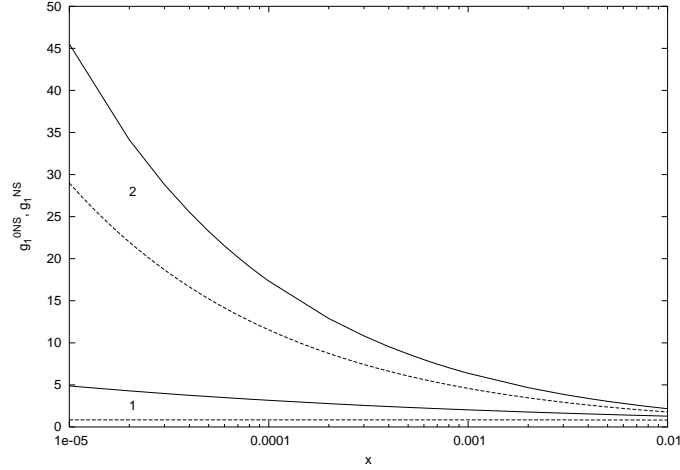


Fig. 1. Input parametrisations g_1^{0NS} (4.8)-(4.9) (dashed) and $g_1^{NS}(x, Q^2 = 10)$ (solid) for these inputs within $\ln^2 x + \text{LO}$ DGLAP approach and for running $\alpha_s(Q^2/z)$.

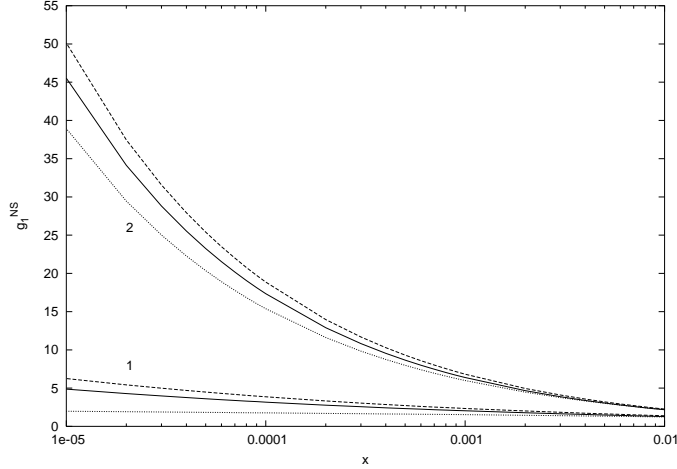


Fig. 2. The small- x predictions for $g_1^{NS}(x, Q^2 = 10)$ within different approximations: LO DGLAP (dotted), $\ln^2 x$ (dashed), unified $\ln^2 x + \text{LO}$ DGLAP (solid). Plots for both inputs (4.8)-(4.9) and running $\alpha_s(Q^2/z)$.

In the last column we give the percentage value $p[\%]$:

$$p = \frac{\Delta I_{BSR}(x_1, x_2, Q^2)}{I_{BSR}(Q^2)} \cdot 100\% \quad (4.11)$$

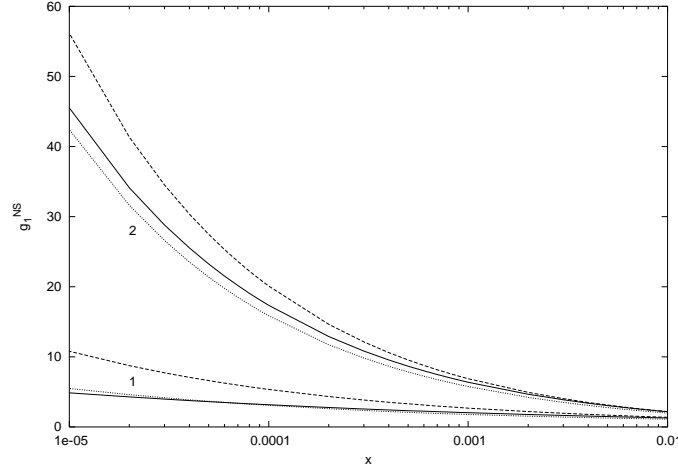


Fig. 3. The small- x predictions for $g_1^{NS}(x, Q^2 = 10)$ within unified $\ln^2 x + \text{LO}$ DGLAP approach for different α_s : $\alpha_s = 0.18$ (dotted), $\alpha_s(Q^2)$ (dashed), $\alpha_s(Q^2/z)$ (solid). Plots for both inputs (4.8)-(4.9).

In Table II we collect results for all possible combinations of approximations and α_s sets: LO DGLAP and $\alpha_s = \text{const} = 0.18$, LO DGLAP and $\alpha_s = \alpha_s(Q^2), \dots, \ln^2 x$ and $\alpha_s = \alpha_s(Q^2/z)$ etc. We present here $\Delta I_{BSR}(0, 3 \cdot 10^{-3}, 10)$, $g_1^{NS}(x = 10^{-6}, Q^2 = 10)$. In the last column the effective slope λ (2.3) at $Q^2 = 10 \text{ GeV}^2$ and small- x [$10^{-6}; 10^{-5}$] is shown. We use again both inputs $g_1^{0NS}(x)$.

x_1	x_2	$\Delta I_{BSR}(x_1, x_2, 10)$	$\varepsilon(x_1, x_2)$	p%
0	$3 \cdot 10^{-3}$	(1) 0.006108	1.4213	2.89
		(2) 0.020668	0.4097	9.80
0	10^{-2}	(1) 0.016050	0.9289	7.61
		(2) 0.040000	0.3336	18.96
10^{-5}	10^{-3}	(1) 0.002457	1.9422	1.16
		(2) 0.010450	0.4574	4.95
10^{-4}	10^{-2}	(1) 0.015672	0.9028	7.43
		(2) 0.037380	0.3214	17.72

Table 1. The small- x contribution to the BSR (4.6) for different input parametrisations (4.8)-(4.9) within $\ln^2 x + \text{LO}$ DGLAP approximation with running $\alpha_s(Q^2/z)$.

From these results one can read that the low- x $g_1^{NS}(x, Q^2)$ values and hence the low- x contributions to the BSR strongly depends on the input parametri-

$g_1^{0NS}(x)$	<i>approach</i>	α_s	$\Delta I_{BSR}(0, 0.003)$	g_1^{NS}	λ
1.Regge	LO	const=0.18	0.003879	2.07	0.06
		$\alpha_s(Q^2)$	0.005742	4.31	0.11
		$\alpha_s(Q^2/z)$	0.004534	2.17	0.04
	ln^2x	const=0.18	0.005614	10.2	0.25
		$\alpha_s(Q^2)$	0.008855	23.9	0.31
		$\alpha_s(Q^2/z)$	0.007043	9.93	0.20
	ln^2x+LO	const=0.18	0.005440	9.75	0.25
		$\alpha_s(Q^2)$	0.008281	21.8	0.30
		$\alpha_s(Q^2/z)$	0.006108	7.36	0.18
2."Toy"	LO	const=0.18	0.017283	88.6	0.40
		$\alpha_s(Q^2)$	0.020543	110	0.40
		$\alpha_s(Q^2/z)$	0.019184	98.0	0.40
	ln^2x	const=0.18	0.019026	113	0.42
		$\alpha_s(Q^2)$	0.023641	161	0.44
		$\alpha_s(Q^2/z)$	0.022175	130	0.41
	ln^2x+LO	const=0.18	0.018756	111	0.42
		$\alpha_s(Q^2)$	0.022712	152	0.43
		$\alpha_s(Q^2/z)$	0.020668	117	0.41

Table 2. $\Delta I_{BSR}(0, 0.003, 10)$, $g_1^{NS}(x = 10^{-6}, 10)$ and λ for both input parametrisations (4.8)-(4.9) within different approaches and α_s .

sation g_1^{0NS} . For the flat Regge form (4.8) $\Delta I_{BSR}(0, 10^{-2}, 10)$ is equal to around 7.6% of the total $I_{BSR} = 0.211$, while for the singular input (4.9) 19.0%. The structure function g_1^{NS} itself at very small- $x = 10^{-6}$ and $Q^2 = 10\text{GeV}^2$ is in a case of $x^{-0.4}$ input about 16 times larger than for the flat one. The value of $\varepsilon(x_1, x_2)$, defined in (4.10) varies from $0.9 \div 1.9$ for the Regge input 1 to $0.3 \div 0.5$ for the singular input 2. The effective slope λ (2.3) describing the small- x behaviour of the structure function g_1^{NS} remains unchanged in a case of the singular input. Namely, the $x^{-0.4}$ shape of the input $g_1^{0NS}(x)$ implies again the same low- x behaviour of the $g_1^{NS}(x, Q^2)$, independently of the Q^2 -evolution approach. Quite different situation occurs for the flat inputs e.g. the Regge one (4.8), where the singular small- x behaviour of the $g_1^{NS}(x, Q^2)$ is totally generated by the QCD evolution with ln^2x terms. Pure double logarithmic ln^2x approach or combined ln^2x+LO DGLAP approximation give the value of λ from 0.2 to 0.3. Only in the pure LO DGLAP analysis we obtain $\lambda \leq 0.1$. It means that the double logarithmic ln^2x effects are better visible in a case of nonsingular inputs. In a case of singular input parametrisations $g_1^{0NS} \sim x^{-\lambda}$ (e.g. $\lambda \sim 0.4$) the

growth of g_1^{NS} at small- x , implied by the $\ln^2 x$ terms resummation, is hidden behind the singular behaviour of g_1^{0NS} , which survives the QCD evolution. Comparing plots from Fig.2 and results from the last column in Table II, one can read that the $\ln^2 x$ resummation gives steep growth of the g_1^{NS} in the small- x region. It is well visible in a case of the Regge input, where $g_1^{NS}(x, Q^2)$ within $\ln^2 x$ or $\ln^2 x + \text{LO DGLAP}$ approaches strongly dominate over that, obtained in pure LO DGLAP approximation. Double logarithmic contributions of the type $(\alpha_s \ln^2 x)^n$, which lead to the strong growth of structure functions at low- x are not included in the DGLAP evolution (LO or NLO). Differences between pure $\ln^2 x$ and $\ln^2 x + \text{LO DGLAP}$ results within the same set of α_s are not very significant. However, pure $\ln^2 x$ approximation overestimate the value of g_1^{NS} and should be accompanied by the LO DGLAP evolution. This is because in the larger- x region, involved in the evolution equation for f^{NS} (3.1), pure $\ln^2 x$ analysis is inadequate. The crucial point in QCD analysis is a treatment of the coupling α_s . The problem of α_s parametrisations in high energy processes has been widely discussed in [9]. Fixed, constance α_s is very convenient in many physical problems. Thus, use of the fixed α_s simplifies the evolution equations for structure functions and enables easy analytical solutions. However, an introduction of the fixed coupling needs a reasonable scale and this is somehow "artificial". Namely, the scale for fixing of α_s is not well defined. In perturbative QCD one should take into account running α_s effects. In this way, usually, the prescription for the running coupling reads $\alpha_s = \alpha_s(Q^2)$. This construction is however accurate only for hard QCD processes, where $x \sim 1$. On the other hand, many interesting QCD processes (e.g. DIS at low- x) are Regge-like. For these cases, with small- x involved, "hard" running $\alpha_s(Q^2)$ is incorrect. Instead of $\alpha_s(Q^2)$ one has to use a modified parametrisation of α_s :

$$\alpha_s = \alpha_s(k_{\perp}^2/\beta) \quad (4.12)$$

where k_{\perp}^2 is the transverse momentum of the ladder parton and β is the standard Sudakov parameter. In our approach this prescription reads as (3.11). From Fig.3 and Table II we are able to compare the predictions for g_1^{NS} at small- x for three α_s parametrisations (3.9)-(3.11). The results for $\alpha_s = \text{const} = 0.18$ and $\alpha_s = \alpha_s(Q^2/z)$ (within the same approach LO or $\ln^2 x$ etc. and with the same input g_1^{0NS}) are similar but significantly smaller than in a case of running $\alpha_s = \alpha_s(Q^2)$. Within $\ln^2 x + \text{LO DGLAP}$ approximation with flat input for "very" running $\alpha_s(Q^2/z)$ ($x < z < 1$), via weaker coupling ($\alpha_s(Q^2/z) < \alpha_s(Q^2)$), the value of $g_1^{NS}(x = 10^{-6}, Q^2 = 10)$ is almost 3 times smaller than for the "hard" running $\alpha_s(Q^2)$. It is a good lesson how choice of the running coupling influences the results in the low- x region. From the experimental SMC data [10] the low- x contribution to the

BSR at $Q^2 = 10\text{GeV}^2$ is equal to

$$6 \int_0^{0.003} g_1^{NS}(x, Q^2 = 10) dx = 0.09 \pm 0.09 \quad (4.13)$$

The above result has been obtained via an extrapolation of g_1^{NS} to the unmeasured region of x : $x \rightarrow 0$. Forms of the polarised quark distributions have been fitted to SMC semi-inclusive and inclusive asymmetries. In the fitting different parametrisations of the polarised quark distributions [15] [16] have been used. The extrapolation of g_1^{NS} to very small- x region depends strongly on the assumption (input parametrisation) made for this extrapolation. In this way present experimental data give only indirectly the estimation of the small- x contribution to the moments of parton distributions. The result (4.13) with a large statistical error and strongly fit-dependent cannot be a final, crucial value. Nevertheless we would like to estimate the exponent λ in the low- x behaviour of $g_1^{NS} \sim x^{-\lambda}$ using the above SMC result for the small- x contribution to the BSR. Assuming the validity of the BSR (4.5) at large $Q^2 = 10\text{GeV}^2$, one can find:

$$\int_0^{x_0} dx g_1^{NS}(x, Q^2) = I_{BSR}(Q^2) - \int_{x_0}^1 dx g_1^{NS}(x, Q^2) \quad (4.14)$$

where x_0 is a very small value of the Bjorken variable. Taking into account the small- x dependence of $g_1^{NS} \sim x^{-\lambda}$ and the experimental data for $\Delta I_{BSR}(0, 0.003, 10)$ one can obtain:

$$C \int_0^{0.003} x^{-\lambda} dx = 0.015 \pm 0.015 \quad (4.15)$$

The constant C can be eliminated from a low- x SMC data [10]:

$$Cx^{-\lambda} = g_1^{n-p}(x, 10) \quad (4.16)$$

Taking different small- x SMC data, we have found $\lambda = 0.37$ ($x = 0.014$); $\lambda = 0.20$ ($x = 0.008$); $\lambda = 0.38$ ($x = 0.005$).

It seems nowadays that the most probably small- x behaviour of g_1^{NS} is

$$g_1^{NS}(x, Q^2) \sim x^{-0.4} \quad (4.17)$$

This results from latest theoretical analyses [9], which take into account the running coupling effects at low- x . It has been shown in [9] that the intercept

λ controlling the power-like small- x behaviour of g_1^{NS} depends on the choice of the parameters n_f (flavour number), Q_0^2 (input scale) and Λ_{QCD} . The maximal value of λ , which gives the maximal contribution to the structure function g_1^{NS} in the perturbative QCD, incorporating $\ln^2 x$ effects, is equal to 0.4. The same value of $\lambda = 0.4$ was obtained in the semi-phenomenological estimation from BSR for lower Q^2 [17]. The polarised (nonsinglet and singlet as well) structure functions are presently the objects of intensive theoretical investigations. Maybe the crucial point for understanding of the small- x behaviour of structure functions is an analysis beyond the leading order $\alpha_s^n \ln^{2n} x$. The resummation of $\alpha_s^{(n+1)} \ln^{2n} x$ terms is studied in [20]. The corrections to g_1^{NS} due to the nonleading terms are on the level of 1% in the accessible at present experimentally x region, but can be larger (up to about 15%) at very small- $x \sim 10^{-5}$. In the situation, when the present experimental data do not cover the whole region of $x \in (0; 1)$, theoretical predictions for e.g. structure functions in the unmeasured low- x region cannot be directly verified. Latest experimental SMC [2], [10] and HERMES [11] data provide results for the BSR from the region $0.003 \leq x \leq 0.7$ and $0.023 \leq x \leq 0.6$ respectively. In the very small- x region exist only indirect, extrapolated results with large uncertainties. Small- x contribution to the Bjorken sum rule resulting from such indirect SMC data analysis is equal to 0.015 ± 0.015 . Large uncertainties of the small- x experimental results disable unfortunately realistic comparison the data with the theoretical predictions. Namely, all our results for $\Delta I_{BSR}(0, 0.003, 10)$ in Table II: from 0.004 (for LO, $\alpha_s = 0.18$, flat input) to 0.024 (for $\ln^2 x$, $\alpha_s(Q^2)$, singular $x^{-0.4}$ input) are in agreement with SMC data (within the total error). Nevertheless, the progress in theoretical [3],[4], [9],[18],[19],[20] and experimental [2], [10],[11] investigations gives hope that our knowledge about structure functions at small- x is getting better.

5. Summary and conclusions

In this paper we have estimated the nonsinglet polarized structure function g_1^{NS} at small- x and also contributions from the small- x region to the Bjorken sum rule. We have used the numerical solutions within unified double logarithmic and DGLAP ($\ln^2 x + \text{LO DGLAP}$) approximation. Our predictions for $g_1^{NS}(x, Q^2)$ and $\Delta I_{BSR}(x_1, x_2, Q^2)$ have been found for two input parametrisations $g_1^{0NS}(x, Q_0^2)$. These parametrisations describe different small- x behaviour of $g_1^{0NS} = g_1^{0(p-n)}$ at Q_0^2 : $g_1^{NS} \sim x^{-\lambda}$. The main conclusion from our analyses is that the structure function g_1^{NS} at small- x and hence also the small- x contribution to the BSR strongly depends on the input parametrisation g_1^{0NS} . The percentage value $\Delta I_{BSR}(0, 10^{-2}, Q^2 = 10)$ of the total BSR ≈ 0.211 varies from 7.6 for the flat Regge input 1 ($\lambda = 0$) to

almost 19 for the singular one 2 ($\lambda = 0.4$). The structure function g_1^{NS} itself at very small- $x = 10^{-6}$ and $Q^2 = 10\text{GeV}^2$ is in a case of $x^{-0.4}$ input about 16 times larger than for the flat one. Double logarithmic $\ln^2 x$ effects, responsible for the strong growth of the structure function in the low- x region, are better visible in a case of nonsingular inputs. In a case of singular input parametrisations $g_1^{0NS} \sim x^{-\lambda}$ (e.g. $\lambda \sim 0.4$) the growth of g_1^{NS} at small- x , implied by the $\ln^2 x$ terms resummation, is hidden behind the singular behaviour of g_1^{0NS} , which survives the QCD evolution. Input parametrisation 2 incorporates latest theoretical investigations, which suggest singular small- x shape of polarised structure functions: $\sim x^{-0.4}$ for the nonsinglet case and even $\sim x^{-0.8}$ for the singlet one. Both these values are indirectly confirmed by fitted experimental HERMES data. Basing on these results, similar extrapolations of the spin dependent quark distributions towards the very low- x region have been assumed in several recent input parametrisations $\Delta q(x, Q_0^2)$. Our results for the small- x contribution $0 \leq x \leq 0.003$ to the BSR are in agreement with the experimental SMC data (for both inputs). However it must be emphasized, that SMC data for the low- x region suffer from large uncertainties. Using SMC data for g_1^{NS} at small- x ($0.14, 5 \cdot 10^{-3}, 8 \cdot 10^{-3}$) we have estimated the exponent λ which governs the low- x behaviour of g_1^{NS} . Thus we have obtained $\lambda = 0.20 \div 0.38$ with large uncertainties. This effective slope λ calculated for low- $x \in [10^{-6}; 10^{-5}]$ from g_1^{NS} in our approach amounts about 0.2 (for running $\alpha_s(Q^2/z)$ and Regge-like flat input). In order to have reliable theoretical predictions for the polarised structure function $g_1^{NS}(x, Q^2)$ we have used unified approach which contains the resummation of the $\ln^2 x$ and the LO DGLAP Q^2 evolution as well. It is because the pure $\ln^2 x$ approximation generates correctly the leading small- x behaviour of the polarised structure function but is inaccurate for larger values of x . Another crucial point of the presented analysis is the role of the running coupling effects. Latest theoretical studies suggest introduction of the running coupling of a form $\alpha_s = \alpha_s(Q^2/z)$ instead of $\alpha_s = \alpha_s(Q^2)$. This is more justified in the small- x region. We have found that the choice of the running coupling significantly influences the results in the low- x region. E.g. the value of $g_1^{NS}(x = 10^{-6}, Q^2 = 10)$ is for "hard" running $\alpha_s(Q^2)$ almost 3 times greater than for the "very" running $\alpha_s(Q^2/z)$ (in a case of nonsingular input g_1^{0NS}). Proper theoretical treatment of the Q^2 evolution of structure functions in the whole (small and large) x region with all essential perturbative leading and even nonleading effects involved should be a subject of further intensive investigations. It is important because of lack of the experimental data from the very small- x region ($x < 0.003$). Agreement of the theoretical predictions e.g. for the BSR with real experimental data at medium and large x may give hope, that for the very interesting small- x region the suitable theoretical results are also reliable.

Acknowledgements

We thank Boris Ermolaev for constructive remarks and useful comments concerning the running coupling effects in the small- x region. We are also grateful to Johannes Blümlein for pointing out the role of nonleading terms in polarised structure functions.

REFERENCES

- [1] J.D.Bjorken, *Phys. Rev.* **148**, 1467 (1966); *Phys. Rev.* **D1**, 1376 (1970).
- [2] SMC Collaboration: D.Adams *et al.*, *Phys. Rev.* **D56**, 5330 (1997).
- [3] J.Kwieciński, *Acta Phys. Pol.* **B27**, 893 (1996).
- [4] J.Bartels, B.I.Ermolaev, M.G.Ryskin, *Z. Phys.* **C70**, 273 (1996); J.Bartels, B.I.Ermolaev, M.G.Ryskin, *Z. Phys.* **C72**, 627 (1996).
- [5] P.D.B.Collins, *An Introduction to Regge Theory and High Energy Physics*, Cambridge University Press, Cambridge 1977.
- [6] M.Glück, E.Reya, M.Stratmann, W.Vogelsang, *Phys. Rev.* **D63**, 094005 (2001).
- [7] G.Altarelli, R.D.Ball, S.Forte, G.Ridolfi, *Acta Phys. Pol.* **B29**, 1145 (1998).
- [8] D.Kotlorz, A.Kotlorz, *Acta Phys. Pol.* **B35**, 705 (2004).
- [9] B.I.Ermolaev, M.Greco, S.I.Troyan, *Nucl. Phys.* **B571**, 137 (2000); hep-ph/0106317; *Nucl. Phys.* **B594**, 71 (2001); *Phys. Lett.* **B522**, 57 (2001); *Phys. Lett.* **B579**, 321 (2004); hep-ph/0404267.
- [10] SMC Collaboration: B.Adeva *et al.*, *Phys. Lett.* **B420**, 180 (1998).
- [11] HERMES Collaboration: K.Ackerstaff *et al.*, *Phys. Lett.* **B404**, 383 (1997); A.Airapetian *et al.*, *Phys. Lett.* **B442**, 484 (1998); K.Ackerstaff *et al.*, *Phys. Lett.* **B464**, 123 (1999).
- [12] S.Forte, L.Magnea, *Phys. Lett.* **B448**, 295 (1999).
- [13] Y.Goto *et al.*, *Phys. Rev.* **D62**, 034017 (2000).
- [14] J.Blümlein, H.Böttcher, *Nucl. Phys.* **B636**, 225 (2002).
- [15] M.Glück, E.Reya, M.Stratmann, W.Vogelsang, *Phys. Rev.* **D53**, 4775 (1996).
- [16] T.Gehrmann, W.J.Stirling, *Phys. Rev.* **D53**, 6100 (1996).
- [17] A.Knauf, M.Meyer-Hermann, G.Soff, *Phys. Lett.* **B549**, 109 (2002).
- [18] B.Badelek, J.Kwieciński, *Phys. Lett.* **B418**, 229 (1998).
- [19] B.Ziaja, *Acta Phys. Pol.* **B32**, 2863 (2001).
- [20] J.Blümlein, A.Vogt, *Phys. Lett.* **B370**, 149 (1996); *Acta Phys. Pol.* **B27**, 1309 (1996); *Phys. Lett.* **B386**, 350 (1996).